ISSN 0915-633X

NATIONAL INSTITUTE FOR FUSION SCIENCE

Stabilities of Regular Motion in the Relativistic Standard Map

Y. Nomura, Yoshi H. Ichikawa and W. Horton

(Received – Jan. 18, 1991)

NIFS-73 Feb. 1991

RESEARCH REPORT
NIFS Series

NAGOYA, JAPAN

STABILITIES OF REGULAR MOTION IN THE RELATIVISTIC STANDARD MAP

Y. Nomura and Y. H. Ichikawa

National Institute for Fusion Science, Nagoya 464-01, Japan

W. Horton

Institute for Fusion Studies, The University of Texas at Austin,

Austin, Texas 78712-1060, U. S. A.

ABSTRACT

Analysis of the relativistic standard map is one of the important problems to understand nonlinear interaction between waves and charged particles in the relativistic dynamics. In the relativistic standard map, in general, chaotic motion is strongly suppressed and regular motion such as periodic orbit plays dominant roles in the phase space. Location of periodic points is predicted by use of symmetry lines of the map. Local stability of periodic points is investigated by introducing the residue of the orbit which characterizes the eigenvalue of the area-preserving map. It is found that the exchange of stable and unstable points takes place at some value of the relativistic parameter. Special behavior of the residue of the Poincare-Birkhoff period-4 points are also examined and related bifurcations are clarified.

Keywords :
relativistic standard map,
chaotic motion, regular motion,
involution decomposition, symmetry lines,
periodic orbits, stability, residue,
Poincare-Birkhoff multifurcation,
period-doubling bifurcation,
period-3 catastrophe

1. INTRODUCTION

In nonlinear dynamical systems, area-preserving maps have been investigated extensively as useful method for characterizing the non-integrable Hamiltonian systems.[1, 2] Especially, non-relativistic acceleration of charged particles by an infinite sequence of constant amplitude longitudinal waves with equally spaced phase velocities is represented by the standard map.[3] This map exhibits regular and chaotic motion and has been studied in various fields of physics. Critical problem of the study of the standard map is a transport process under the coexistance of regular motion and chaos.[4-7] Recently, Chernikov et al.[8] introduced the relativistic generalization of the standard map. They have found that the chaotic motion is restricted to the vicinity of the fixed points and the breakup of last KAM torus occurs at higher wave amplitude than that for the standard map.

In this work, we clarify the relativistic effects on the nonlinear motion of particles by varying the wave phase velocity in a wide range.[9] In the ultra-relativistic case, chaos is very weak compared to the regular motion such as KAM tori or periodic orbits. In order to specify the periodic orbits, we carry out symmetry analysis[10-13] of the relativistic standard map. Stability of the periodic orbit is worked out in terms of the characteristic multiplier or the residue[4] of the orbit. Finally, the Poincare-Birkhoff multifurcation of periodic orbits from stable periodic points (island around island) is considered.

2. REGULAR MOTION AND CHAOS IN THE RELATIVISTIC STANDARD MAP

Relativistic motion of charged particles in an infinite sequence of electrostatic waves with constant amplitude and equally spaced phase velocities is described by the relativistic standard map[8, 9] in the normalized form :

$$P_{n+1} = P_n + F(X_n), \quad X_{n+1} = X_n + G(P_{n+1}), \tag{1}$$

$$F(X) = -(K/2\pi)\sin(2\pi X), \quad G(P) = P/[1 + \beta_P{}^2 P^2]^{1/2}$$

where K is the stochastic parameter which corresponds to the wave amplitude and the relativistic parameter β_P is defined as the ratio of phase velocity v_0 of the slowest wave to the speed of light c, $\beta_P \equiv v_0/c$. In the limiting case of $\beta_P \to 0$, the map (1) is reduced to the usual standard map. Fundamental properties of the relativistic standard map such as the stability of fixed points or the Poincare-Birkhoff period-p/q multifurcation condition have been derived in Ref. 9).

Particle trajectories in the relativistic standard map are shown in Fig. 1 for various values of β_P at K = 1.3. In these figures, particles are initially distributed uniformly at P = 0 and advanced according to the map (1) till n = 5000. For weekly relativistic case, $\beta_P \ll 1$, diffusion of particles at low momentum region is qualitatively the same as that in the standard map. The

stochastic region, however, is bounded by an invariant KAM surface at high momentum and global chaos is suppressed. As the parameter β_P increases, the maximum attainable momentum decreases rapidly and the particle diffusion is restricted to a thin layer.

In the ultra-relativistic case, $\beta_P \gg 1$, particle trajectory becomes quite regular. Secondary island chains with very high period are formed inside the separatrix KAM surface and the stochastic layer in the peripheral region of island chains is observed. In order to characterize this regular structure of the phase space, it is useful to analyze symmetry property of the map introduced by Birkhoff.[10] In the next section, we identify the periodic orbits by means of symmetry analysis.

3. SYMMETRY OF THE RELATIVISTIC STANDARD MAP

We consider a 2D area-preserving map T of the form given by Eq. (1). A map T is called reversible[14-16] if there exists an involution I_0 which satisfies the relation

$$T \cdot I_0 \cdot T = I_0 , \qquad I_0 \cdot I_0 = Id. \tag{2}$$

This relation indicates that the reversible map can be expressed as the product of two involutions:

$$T = I_1 \cdot I_0 , \qquad I_1 \cdot I_1 = Id. , \qquad I_1 \equiv T \cdot I_0 \tag{3}$$

and the inverse transformation T^{-1} is given by

$$T^{-1} = I_0 \cdot I_j \tag{4}$$

If we define I_j as the jth iteration of the map T on the involution I_0, $I_j \equiv T^j \cdot I_0$, we immediately confirm that I_j is also an involution. Ensemble of I_j and T^k for arbitrary integers j and k forms a discrete infinite group with the relationships:

$$I_j \cdot I_k = T^{j-k}, \quad T^j \cdot I_k = I_{j+k}, \quad I_j \cdot T^k = I_{j-k} \tag{5}$$

It can be shown that the fixed points of the involution I_j form a line Γ_j which is called as its symmetry line,

$$\Gamma_j : \{ R \mid I_j R = R \} . \tag{6}$$

Therefore, the first equation of (5) defines that the intersection of Γ_j and Γ_k determines periodic points of T, whose period N divides $| j - k |$. From the second and the third equations of (5), we can deduce that the symmetry lines are transformed by T^N into other symmetry lines : $T^N \cdot \Gamma_j = \Gamma_{2N+j}$. This relation enables us to facilitate the construction of symmetry lines of arbitrary order.

Since the transformation function F is anti-symmetric with respect to the space inversion, $F(-X) = - F(X)$, the map (1) is expressed as the composition of the following involutions :

$$I_0 : \quad P' = P + F(X), \qquad X' = -X$$

$$I_1 : \quad P' = P, \qquad X' = -X + G(P) \tag{7}$$

Symmetry lines of these two involutions are given by

$$\Gamma_0 : \quad X = 0, \qquad \Gamma_1 : \quad 2X - G(P) = 0 \tag{8}$$

A factorization of the map into two involutions is not unique. Anti-symmetricity of the function G with respect to momentum inversion, $G(-P) = -G(P)$, gives rise to another involution decomposition $T = J_1 \cdot J_0$,

$$J_0 : \quad P' = -P, \qquad X' = X - G(P)$$

$$J_1 : \quad P' = -P + F[X - G(P)], \tag{9}$$

$$X' = X - G(P) - G[P - F\{X - G(P)\}]$$

This type of factorization defines momentum inversion symmetry as

$$\gamma_0 : \quad P = 0, \qquad \gamma_1 : \quad 2P - F[X - G(P)] = 0 \tag{10}$$

Figure 2 shows superposition of families of symmetry lines on the phase portrait of the map (1) for $K = 1.3$ and $\beta_P = 4\pi$. It can be

found in Fig. 2(a) that the space inversion symmetry lines become parallel at high momentum, which indicates that phase increase of particles is almost constant for ultra-relativistic case. Momentum inversion symmetry lines in Fig. 2(b) are asymptotic to the separatrix KAM surface. In both figures, intersections of symmetry lines determine stable and unstable periodic orbits.

3. STABILITY OF PERIODIC ORBITS

In the relativistic standard map, stable and unstable periodic orbits are often exchanged at certain values of β_p. Typical examples of this exchange are demonstrated in Figs. 3 and 4 respectively for K=3.3 and 6.4717. In Fig. 3(a), period-4 orbit whose one point lies on the X-axis is stable and the orbit located on the P-axis is unstable. By increasing the relativistic parameter, stable period-4 points turn into unstable and phase shift of island chain occurs as seen in Fig. 3(b). In Figs. 4(a) and (b), phase shift of pairs of period-3 island and period-4 island is clearly found.

In order to examine this exchange, we study the local stability of periodic orbits.[17] Since a periodic orbit of period n is considered as a fixed point of T^n, its stability is determined by the eigenvalue of a matrix L obtained by linearizing T^n about one of its points. Owing to the area preserving property of the map T, characteristic equation for the eigenvalues λ (called the characteristic multipliers) is expressed in terms of the trace of L

$$\lambda^2 - \mathrm{Tr}(L)\lambda + 1 = 0 \tag{11}$$

Thus the stability condition is

$$|\mathrm{Tr}(L)| < 2 \tag{12}$$

In order to divide the stability of periodic orbit, it is practical to introduce the residue R of an orbit defined by

$$R \equiv [2 - \mathrm{Tr}(L)]/4 \tag{13}$$

Then, the characteristic multipliers are given by

$$\lambda = 1 - 2R \pm 2[R(R-1)]^{1/2} \tag{14}$$

The orbit is stable for $0 < R < 1$ and called elliptic. If $R < 0$, the orbit is directly unstable and called as hyperbolic without reflection. For $R > 1$, the orbit is inversely unstable and called hyperbolic with reflection. The eigenvalues are degenerate for $R = 0$ and 1, i.e. $\lambda = 1$ and -1 respectively. In these cases, the orbit is parabolic and topological change is possible through these cases. The latter case is known as period doubling bifurcation.

Now we consider the stability of period-3 and period-4 orbits bifurcated from the origin by means of the residue. For period-3 orbits, there exist two types of solutions. Locations of these points are predicted by symmetry analysis described in the

preceding section. Firstly, an orbit whose one point lies on the X-axis can be determined by the intersection of momentum inversion symmetry lines, γ_0 and γ_3 :

$$2F(X_0) + F\,[X_0 + G\,\{\,F(X_0)\}\,] = 0\,, \quad P_0 = 0 \tag{15}$$

The residue of this orbit is given by

$$R^{(3)}\ (X_0, P_0=0)$$

$$= -\tfrac{1}{4}\,[2F'(X_0) + F'\,\{X_0 + G(F(X_0))\}\ \{1+G'(F(X_0))F'(X_0)\ \}\ ]$$

$$\times\,[2G'(F(X_0)) + G'(0)\ \{1+G'(F(X_0))F'(X_0)\ \}\ ] \tag{16}$$

The other type of orbit whose one point lies on the P-axis is determined by the space inversion symmetry lines, Γ_0 and Γ_3 :

$$2G(P_0) + G\,[P_0 + F\,\{G(P_0)\ \}\ ] = 0, \quad X_0 = 0 \tag{17}$$

In this case, the residue is expressed as

$$R^{(3)}\ (X_0=0, P_0)$$

$$= -\tfrac{1}{4}\,[2G'(P_0) + G'\,\{P_0 + F(G(P_0))\}\ \{1+F'(G(P_0))G'(P_0)\ \}\ ]$$

$$\times\,[2F'(G(P_0)) + F'(0)\ \{1+F'(G(P_0))G'(P_0)\ \}\ ] \tag{18}$$

It is noted that these two orbits exist when the stochastic parameter K exceeds 3 which is nothing but the Poincare-Birkhoff multifurcation condition.

Similarly, location of period-4 orbit which lies on the X-axis is specified by the intersection of symmetry lines γ_0 and γ_4 :

$$F(X_0) + F\left[X_0 + G\{F(X_0)\}\right] = 0, \quad P_0 = 0 \tag{19}$$

Because the function F is sinusoidal, Eq.(19) is reduced to the following two cases.

a) $$2X_0 + G\{F(X_0)\} = 0 \tag{20}$$

This period-4 pair exists at $(0, X_0)$, $[F(X_0), -X_0]$, $(0, -X_0)$, and $[-F(X_0), X_0]$. The orbit is symmetric with respect to the origin and the existing condition is $K>2$. Thus, this is identified as the Poincare-Birkhoff pair. The residue for this branch is given by

$$R^{(4)}(X_0, P_0=0)$$

$$= -\tfrac{1}{4}F'(X_0)\left[2 + G'(F(X_0))\right]\left[2 + G'(0)F'(X_0)\right]$$

$$\times \left[2G'(F(X_0)) + G'(0)\{2+G'(F(X_0))F'(X_0)\}\right] \tag{21}$$

The other type of reduction is possible for Eq.(19):

b) $G\{F(X_0)\} = m + 1/2 \quad (m:\text{integer})$ (22)

Positions of this pair are $(0, X_0)$, $[F(X_0), X_0+\frac{1}{2}]$, $(0, X_0+\frac{1}{2})$ and $[-F(X_0), X_0]$. This period-4 pair is asymmetric with respect to the origin. Because the relativistic standard map is symmetric with respect to the origin, two pairs of period-4 orbits of this type always appear when the following bifurcation condition is satisfied

$$K\left[\left(m+\tfrac{1}{2}\right)^{-2} - \beta_P{}^2\right]^{1/2} > 2\pi \tag{23}$$

The residue of this orbit is calculated as

$$R^{(4)}(X_0, P_0=0)$$

$$= -\tfrac{1}{4}\, G'(F(X_0))F'^2(X_0)$$

$$\times \left[G'(F(X_0))G'^2(0)\, F'^2(X_0) - 4\,\{G'(0)+ G'(F(X_0))\}\right] \tag{24}$$

In addition to the above-mentioned orbits, there exists another type of period-4 orbit whose one point lies on the P-axis. The location is predicted by the symmetry lines Γ_0 and Γ_4 as

$$G(P_0) + G\left[P_0 + F\{G(P_0)\}\right] = 0, \quad P_0 = 0 \tag{25}$$

In contrast to the cases mentioned above, this equation is uniquely reduced to

$$2P_0 + F\{G(P_0)\} = 0 \tag{26}$$

and the orbit exists when $K > 2$ (Poincare-Birkhoff condition). The residue of this orbit is given by

$$\begin{aligned} R^{(4)}\ (X_0=0, P_0) &= -\tfrac{1}{4} G'(P_0)\,[2 + F'(G(P_0))]\ [2 + F'(0)G'(P_0)] \\ &\quad \times [2F'(G(P_0)) + F'(0)\{2+F'(G(P_0))G'(P_0)\}] \end{aligned} \tag{27}$$

Figures 5 and 6 show respectively the residue of period-3 and period-4 orbits at $K = 3.3$. In Fig. 5, it is seen that the residues of both period-3 orbits become zero at $\beta_P = 2.40$ and the stability exchange takes place at this value. As for the period-4 in Fig. 6, all of the pairs are unstable at $\beta_P = 0$, i. e., the asymmetric branch indicated by (b) is inversely and the Poincare-Birkhoff pairs are directly unstable. As the value β_P increases, the residue of the asymmetric branch decreases and those of the Poincare-Birkhoff Pairs increase. The asymmetric pairs turn into stable and are absorbed by the Poincare-Birkhoff pair indicated by (a) at $\beta_P = 0.612$ where the condition (23) is just equal to zero and $F'(X_0) = 0$ in Eqs. (21) and (24). The residue of the Poincare-

Birkhoff pair on the X-axis increases to 1 and then decreases. At $\beta_P = 2.44$, residues of both Poincare-Birkhoff pairs become 0 simultaneously and the stability exchange occurs which agrees with the observation in Fig. 3.

In Figs. 7 and 8, residues of period-3 and period-4 orbits at K = 6.4717 are demonstrated, respectively. In contrast to the case of K = 3.3, the period-3 orbits are fairly unstable and the stable island exists in a very narrow range of β_P. The stability exchange takes place at $\beta_P = 2.34$ which confirms the island shift in Fig. 4. The residues of period-4 pairs vary in a very complicated manner. In Fig. 8, we see that all pairs are directly unstable at $\beta_P = 0$. As β_P increases, asymmetric pair becomes stable firstly; however, it soon becomes inversely unstable and then its residue decreases and turns stable again. This pair merges with the Poincare-Birkhoff pair at $\beta_P = 1.749$. The Poincare-Birkhoff pair located on the X-axis is stable for $1.749 < \beta_P < 2.28$ and the residue comes up to 1 and then falls again. At $\beta_P = 2.28$, both of Poincare-Birkhoff pairs take the value $R^{(4)} = 0$ and phase shift of period-4 island seen in Fig. 4 is explained by this fact. As β_P increases further, the pair on the P-axis becomes stable and its residue comes up to 1 and then goes down again. The special behavior of the residue of the Poincare-Birkhoff period-4 orbits is treated in the next section with relation to the multifurcation from period-4 points.

4. POINCARE-BIRKHOFF MULTIFURCATION FROM PERIOD-4 ORBIT

In the preceding section, we have found that the residue of period-4 orbit increases to unity and then falls again as β_P increases. We should aware that stable orbits with the same value of residue but different β_P exhibit distinct behaviors. One example is the cases of $R^{(4)} = 0$; at the small value of β_P we see the merging of asymmetric pairs and at the large β_P stability exchange occurs. In Fig.9, phase portrait near the period-4 points on the X-axis is shown for K = 3.3 and (a) $\beta_P = 0.933$ and (b) $\beta_P = 1.57$. In both cases period-4 orbits have residues $R^{(4)} \sim 0.75$. In Fig. 9(a) we can recognize that the period-3 catastrophe arises and the original islands are squeezed into the periodic point by the unstable period-3 orbit. On the other hand in Fig. 9(b), we see the multifurcation of two pairs of period-3 orbits. For $R^{(4)} \sim 1$, at which period doubling begins usually, two pairs of period-2 orbits are multifurcated as shown in Fig. 10.

We will analyze these different behaviors following J. M. Greene et. al.[17] As was studied in Sec. 3, the Poincare-Birkhoff pairs are symmetric with respect to the origin. Thus $(0, X_0)$ and $(0, -X_0)$ are regarded as the same points. In this case, the Poincare-Birkhoff period-4 sequence has a square root map. An introduction of the residue $R^{(2)}$ of T^2 map

$$R^{(2)}\ (0, X_0) = R^{(2)}\ (0, -X_0)$$

$$= -\tfrac{1}{4}F'(X_0)\ [\ 2G'(0) + 2G'(F(X_0)) + G'(0)G'(F(X_0))F'(X_0)\ ] \quad (28)$$

leads to the following expression for $R^{(4)}$

$$R^{(4)} = 4R^{(2)}\ (1 - R^{(2)}\ ) \quad (29)$$

which has a maximum of 1 (at $R^{(2)} = \tfrac{1}{2}$).

Figure 11 shows the values of $R^{(2)}$ and $R^{(4)}$ for the Poincare-Birkhoff pair on the X-axis at K = 3.3. It is found that the residue $R^{(2)}$ is monotonically decreasing with β_P. In the stable elliptic case, the eigenvalues 〔Eq.(14)〕 are expressed in terms of rotation number ρ as

$$\lambda = \exp(\ \pm i2\pi\rho), \quad 2\pi\rho \equiv \cos^{-1}(1 - 2R) \quad (30)$$

When the residue passes through the values

$$R_{p/q} = \sin^2(\ \pi p/q\ ), \quad p, q : \text{coprime integers} \quad (31)$$

the Poincare-Birkhoff islands of q times the original period are born. At $\beta_P = 0.612$, where the asymmetric branch is bifurcated, residues are $R^{(4)} = 0$ and $R^{(2)} = 1$ so that this corresponds to p/q = 1/2 (period doubling) bifurcation for T^2 map and 2/2 (asymmetric) bifurcation for T^4 map. At $\beta_P = 0.933$, $R^{(2)} = R^{(4)} = 3/4$ and the

value p/q is 1/3 for T^2 and 2/3 for T^4. Thus the special case of period-3 catastrophe takes place as observed in Fig. 9(a). On the other hand at $\beta_P = 1.57$, the value $R^{(4)}$ is 3/4 but $R^{(2)} = 1/4$ which corresponds to the 1/6 multifurcation for T^2 and the 2/6 multifurcation for T^4. Therefore two pairs of period-3 islands turn up in Fig. 9(b) rather than period-3 catastrophe. Finally at $\beta_P = 1.26$, $R^{(4)}$ approaches 1 and $R^{(2)}$ passes through 1/2, which is typically the 1/4 multifurcation for T^2 map and 2/4 for T^4. These 4-cycles are recognized as two pairs of period-2 in Fig. 10.

We have discussed the Poincare-Birkhoff multifurcation in connection with the residue of T^2 map. The special case of $R^{(2)} = 3/4$ (corresponding to $\lambda^3 = 1$) is known as period-3 catastrophe or squeeze effect. In this case, period-3 pairs should appear at some value of β_P. In Fig. 12, we see clearly the anomalous onset of period-3 pairs at $\beta_P = 0.9676$. The onset condition can be obtained by expanding the T^2 map around the equilibrium point and retaining the lowest order nonlinear term.[12] As a result the onset condition is expressed by using $R^{(2)}$:

$$R^{(2)} > 1/\sqrt{2} \tag{32}$$

This condition coincides with the value of $R^{(2)}$ at $\beta_P = 0.9676$.

5. CONCLUDING REMARK

Particle acceleration in the relativistic standard map is studied and it is found that the relativistic effects suppress the chaotic motion of particles. For the waves whose phase velocities extremely exceed the speed of light, particle trajectory becomes regular. In this case, periodic orbits play dominant role in the phase space and the stochasticity occurs around the secondary island chains. In order to obtain critical information on the periodic orbits, we carry out the symmetry analysis and construct families of space inversion and momentum inversion symmetry lines. Space inversion symmetry lines exhibit the constant phase increase of particle motion. These two families of symmetry lines predict stable and unstable periodic orbits of arbitrary period.

In the relativistic standard map, stable and unstable periodic orbits are often exchanged when the relativistic parameter β_P takes a certain value. Corresponding phase shift of island chains are observed in numerical calculation. In order to clarify this exchange, we examine local stability of periodic orbits by introducing the concept of residue which characterizes the eigenvalue of the area-preserving map. We have found that the exchange of stabilities for period-3 pairs takes place at $R^{(3)} = 0$. In the case of period-4 orbit, however, the residue $R^{(4)}$ changes much more complicatedly than $R^{(3)}$ for period-3. Firstly, at lower value of β_P with $R^{(4)} = 0$, we have shown the bifurcation of asymmetric period-4 pairs. As β_P increases, residue of the

Poincare-Birkhoff pair located on the X-axis increases to unity and then falls again. After that, residues of Poincare-Birkhoff pairs of both on the X- and P-axes become 0 at the same time. At this value of β_P, stability exchange occurs.

The special behavior of $R^{(4)}$ is analyzed by means of the residue of T^2 map in connection with the Poincare-Birkhoff multifurcation. It is shown that the bifurcation of asymmetric period-4 pairs are regarded as period-doubling bifurcation when considered as periodic points of T^2. Different types of the behavior of period-3 island around period-4 points are seen in Figs. 9 (a) and (b) when $R^{(4)} = 3/4$. For the case of Fig. 9(a), the value $R^{(2)}$ is 3/4 and the exceptional case of period-3 catastrophe arises. On the other hand, in Fig. 9(b), $R^{(2)}$ is 1/4 and two pairs of period-3 islands are multifurcated from period-4 points. If the value $R^{(4)}$ takes its maximum value of 1, $R^{(2)}$ passes through 1/2 and correspondingly two pairs of period-2 orbits are multifurcated. Finally, anomalous onset of period-3 orbits near the period-3 catastrophe is worked out and the onset condition is found consistent with the numerical observation.

In the analysis of stability, we have restricted ourselves to the periodic orbits of low period. The formulation, however, is applicable to higher periodic orbits. Numerical study of the map shows that exchange of stability occurs very frequently for higher periodic orbits. Stabilities of higher periodic orbits are future problems to be discussed.

ACKNOWLEDGEMENT

The authors wish to express their thanks to Prof. K. Tanikawa at National Astronomical Observatory for discussion on the symmetry lines and related stability.

REFERENCES

1. A. J. Lichtenberg and M. A. Liebermann, Regular and Stochastic Motion, Applied Mathematical Sciences 38 (Splinger-Verlag, New York, 1983).
2. G. M. Zaslavsky, Chaos in Dynamical Systems (Harwood, New York, 1985).
3. B. V. Chirikov, Phys. Rep. 52, 265 (1979).
4. J. M. Greene, J. Math. Phys. 20, 1183 (1979).
5. R. S. Mackay, J. D. Meiss and I. C. Percival, Physica 13 D, 55 (1984).
6. J. D. Meiss, J. R. Cary, C. Grebogi, J. D. Crawford, A. N. Kaufman and H. D. I. Abarbanel, Physica 6D, 375 (1983).
7. Y. H. Ichikawa, T. Kamimura and T. Hatori, Physica 29 D, 247 (1987).
8. A. A. Chernikov, T. Tel, G. Vattay and G. M. Zaslavsky, Phys. Rev. A 40, 4072 (1989).
9. Y. Nomura, Y. H. Ichikawa and W. Horton, Kakuyugo Kenkyu 64, 347 (1990). [in Japanese]
10. G. D. Birkhoff, Dynamical Systems (AMS Colloquium Publications,

Vol. IX, 1927) p. 186.

11. E. Pina and L. J. Lara, Physica 26 D, 369 (1987).
12. Y. H. Ichikawa, T. Kamimura, T. Hatori and S. Y. Kim, Prog. Theor. Phys. Suppl. No. 98, 1 (1989).
13. R. de Vogelaere, Contribution to the Theory of Nonlinear Oscillations, S. Lefschetz ed. (Princeton Univ. Press, New Jersey, 1958) Vol. IV, p. 53.
14. G. R. W. Quispel and J. A. G. Roberts, Phys. Lett. A132, 161 (1988).
15. G. R. W. Quispel and J. A. G. Roberts, Phys. Lett. A135, 1183 (1989).
16. G. D. Birkhoff, Dynamical Systems (AMS Colloquium Publications, Vol. IX, 1927) p. 115.
17. J. M. Greene, R. S. Mackay, F. Vivaldi and M. J. Feigenbaum, Physica 3D, 468 (1981).

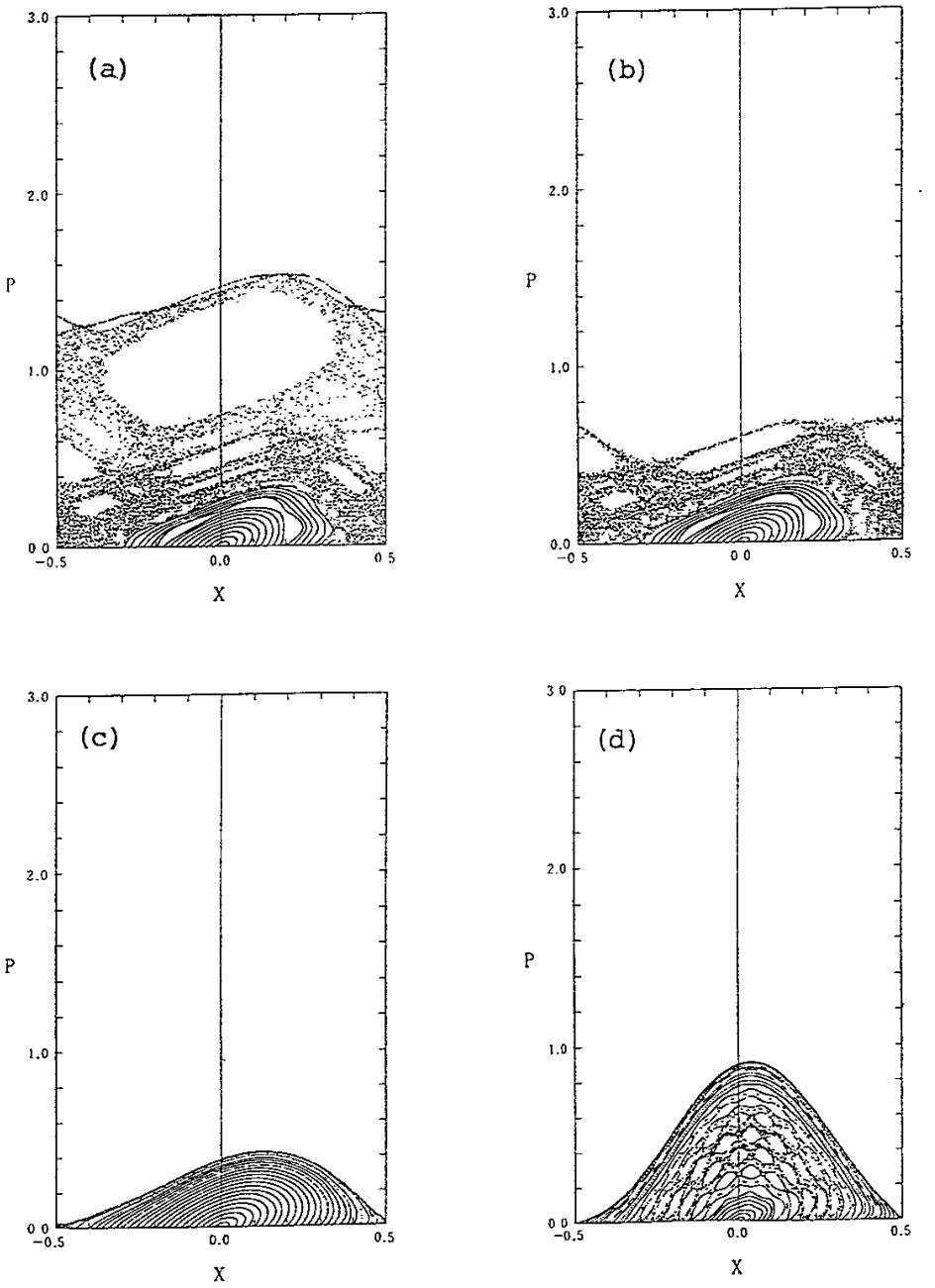

Fig. 1 Particle trajectory in the relativistic standard map. The relativistic parameters are (a) $\beta_P = 0.1\ \pi$, (b) $\beta_P = 0.2\ \pi$, (c) $\beta_P = \pi$ and (d) $\beta_P = 4\ \pi$.

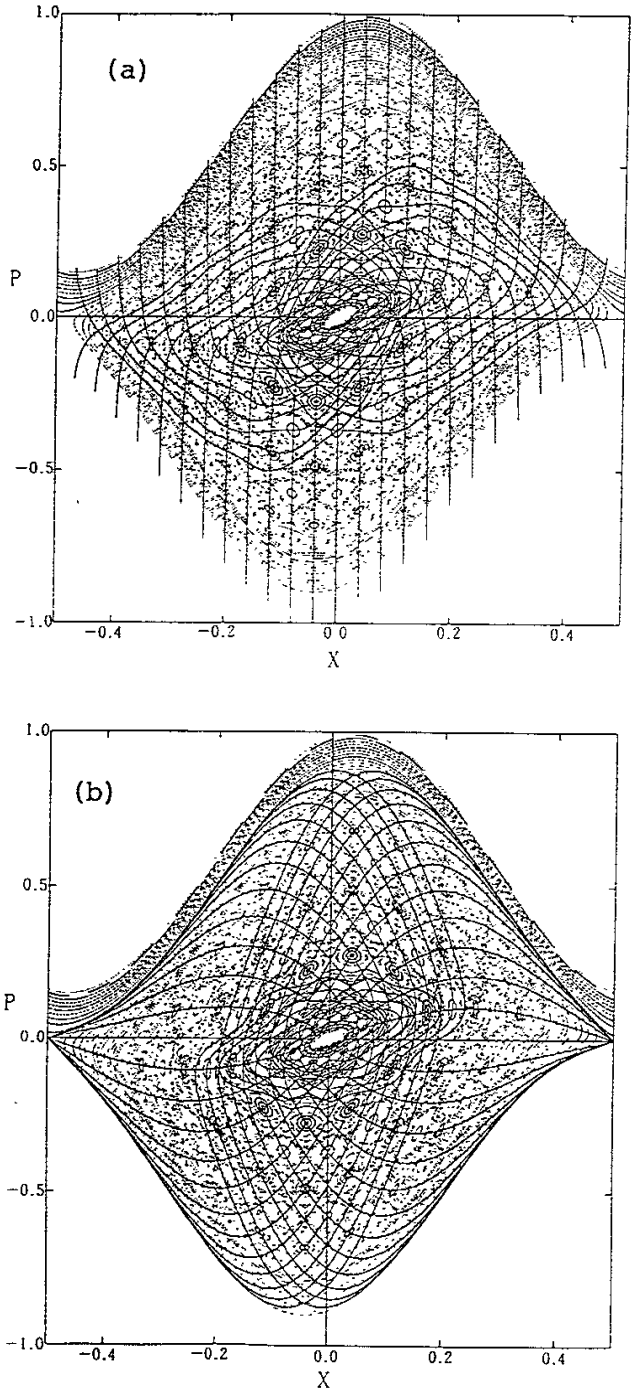

Fig. 2 Superposition of (a) space inversion symmetry lines and (b) momentum inversion symmetry lines on the phase portrait of the relativistic standard map at K = 1.3 and $\beta_P = 4\pi$.

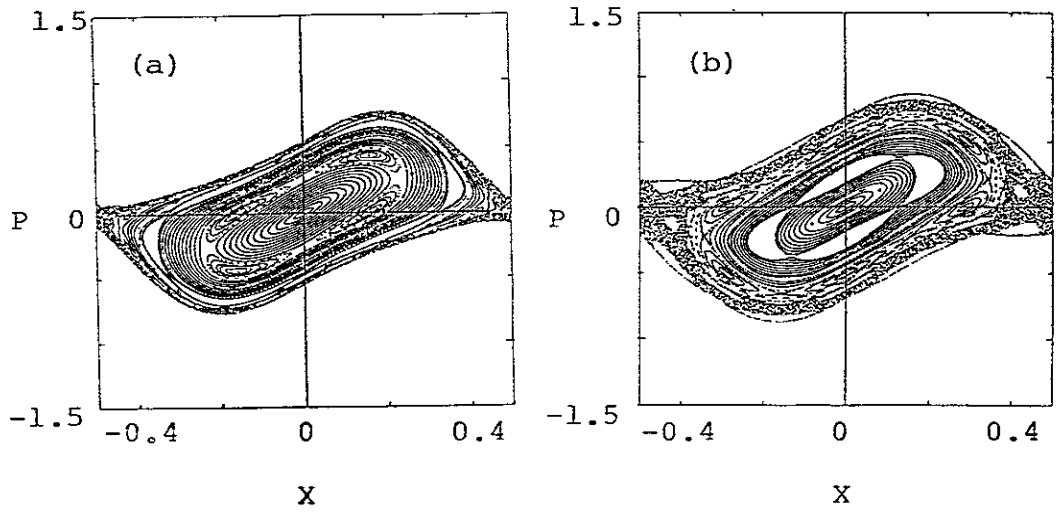

Fig. 3 Phase shift of period-4 islands between (a) β_P = 2.20 and (b) β_P = 2.83 at K = 3.3.

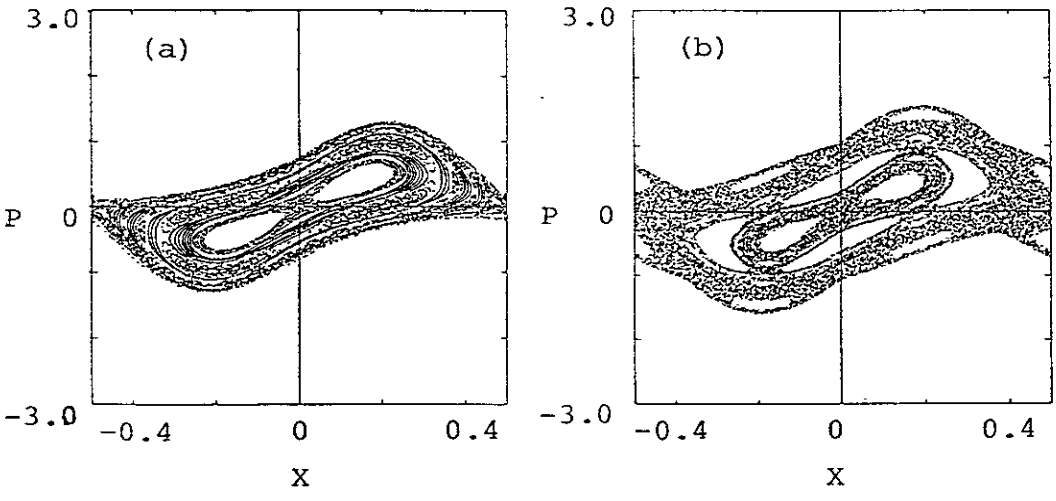

Fig. 4 Phase shift of period-3 and period-4 islands between (a) β_P = 2.20 and (b) β_P = 2.51 at K = 6.4717.

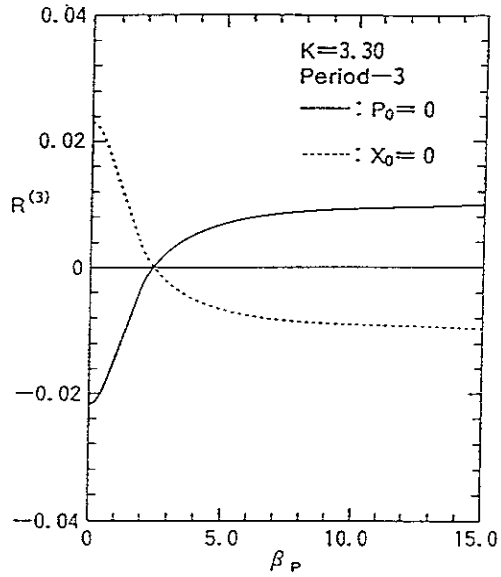

Fig. 5 Residue of period-3 orbit at K = 3.3.

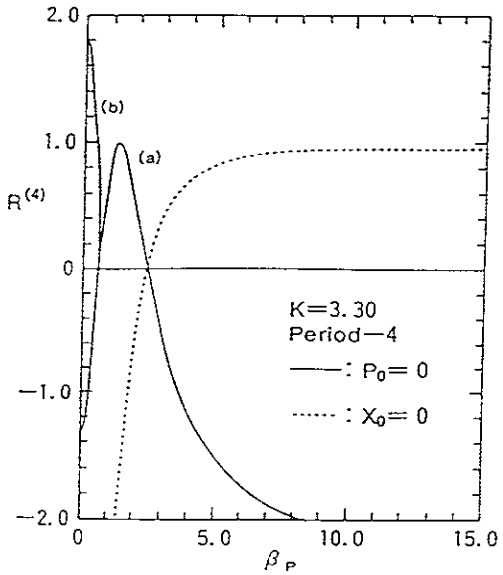

Fig. 6 Residue of period-4 orbit at K = 3.3.

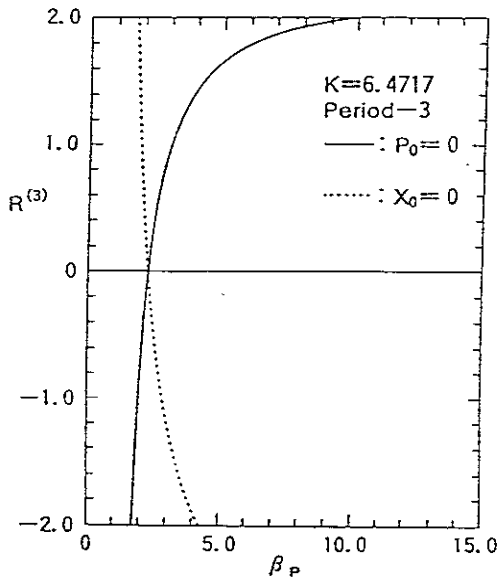

Fig. 7 Residue of period-3 orbit at K = 6.4717.

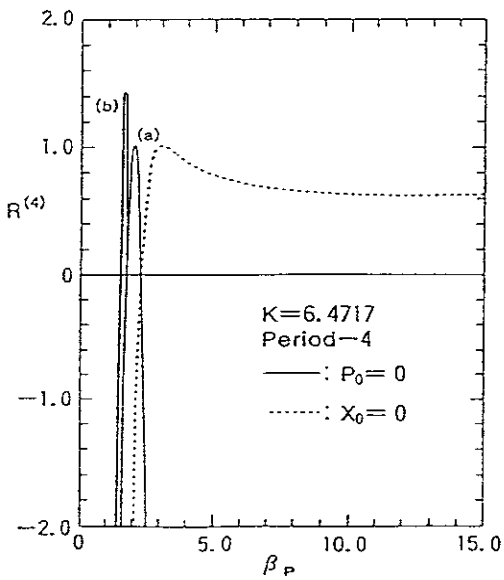

Fig. 8 Residue of period-4 orbit at K = 6.4717.

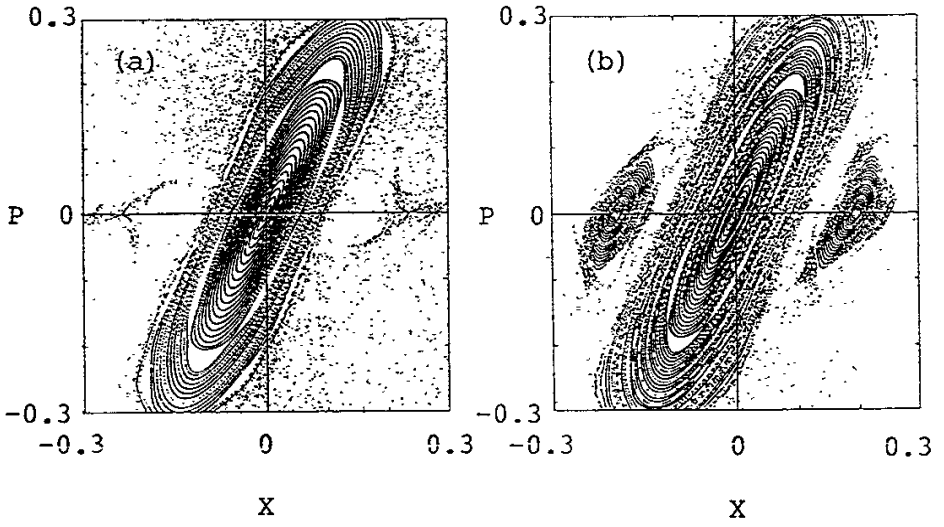

Fig. 9 Multifurcation of period-3 pairs at K = 3.3.
(a) period-3 catastrophe at β_P = 0.933 and (b) two pairs of period-3 islands at β_P = 1.57.

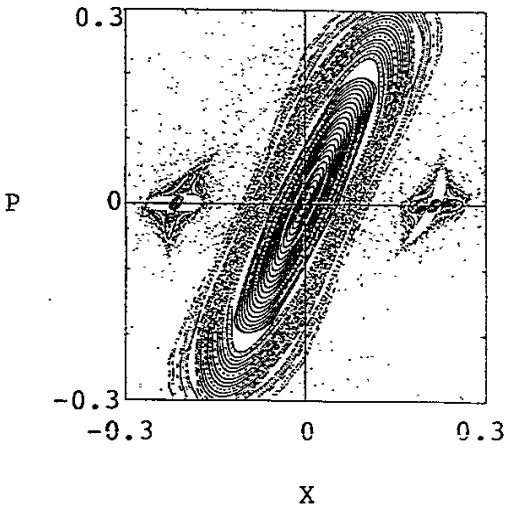

Fig. 10 Multifurcation of two pairs of period-2 orbits at K = 3.3 and β_P = 1.26.

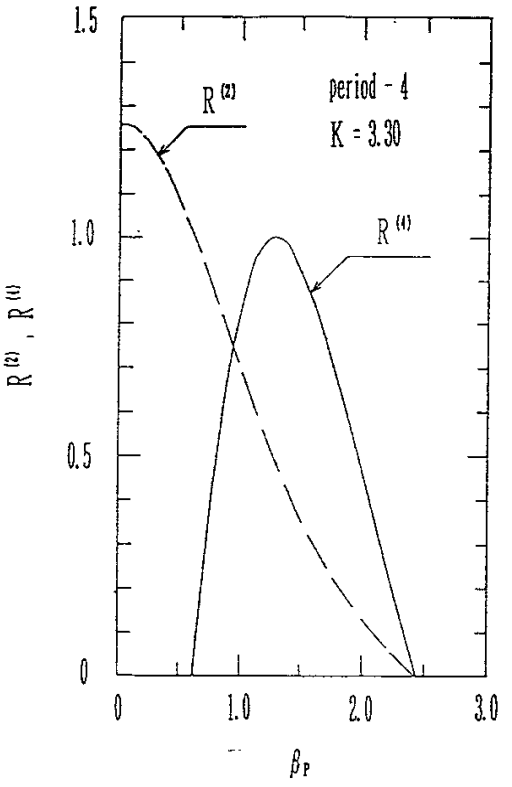

Fig. 11 Residues $R^{(2)}$ and $R^{(4)}$ for the Poincare-Birkhoff period-4 orbit on the X-axis at K = 3.3.

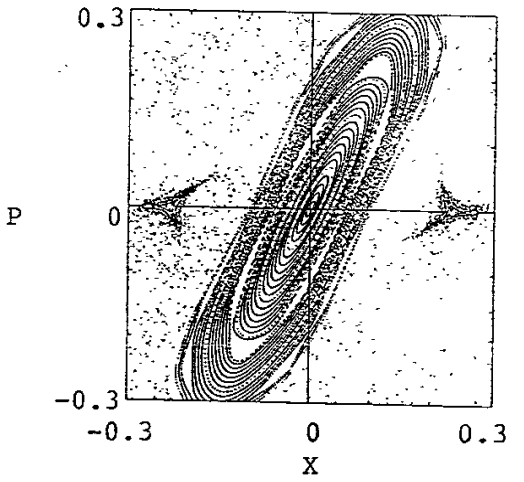

Fig. 12 Onset of period-3 orbit at K = 3.3 and β_P =0.9676.

Recent Issues of NIFS Report

NIFS-24 S.I. Itoh, N. Ueda, and K. Itoh, *Simulation Study of Scalings in Scrape-Off Layer Plasma by Two Dimensional Transport Code* ; Mar. 1990

NIFS-25 B. Bhattacharya, T. Watanabe and Kyoji Nishikawa, *Single Particle and Fluid Picture for Ponderomotive Drift in Nonuniform Plasmas*; Apr. 1990

NIFS-26 K. Ida, S. Hidekuma, Y. Miura, T. Fujita, M. Mori, K. Hoshino, N. Suzuki, T. Yamaguchi and JFT-2M Group, *Edge Electron Field Profiles of H-mode Plasmas in JFT-2M Tokamak* ; Apr. 1990

NIFS-27 N. Nakajima and M. Okamoto, *Beam-Driven Currents in the 1/ v Regime in a Helical System* ; Apr. 1990

NIFS-28 K. Itoh, K. Nagasaki and S.I. Itoh, *Heat Deposition on the Partial Limiter* ; Apr. 1990

NIFS-29 S.-I. Itoh A. Fukuyama adn K. Itoh, *Fokker-Plank Equation in the Presence of Anomallous Diffusion* ; May. 1990

NIFS-30 K. Yamazaki, O. Motojima, M. Asao, M. Fujiwara and A. Iiyoshi, *Design Scalings and Optimizations for Super-Conducting Large Helical Devices* ; May 1990

NIFS-31 H. Sanuki, T. Kamimura, K. Hanatani, K. Itoh and J. Todoroki, *Effects of Electric Field on Particle Drift Orbits in a l =2 Torsatron* ; May 1990

NIFS-32 Yoshi H. Ichikawa, *Experiments and Applications of Soliton Physics*; June 1990

NIFS-33 S.-I. Itoh, *Anomalous Viscosity due to Drift Wave Turbulence* ; June 1990

NIFS-34 K. Hamamatsu, A. Fukuyama, S.-I. Itoh, K. Itoh and M. Azumi, *RF Helicity Injection and Current Drive* ; July 1990

NIFS-35 M. Sasao, H. Yamaoka, M. Wada and J. Fujita, *Direct Extraction of a Na- Beam from a Sodium Plasma* ; July 1990

NIFS-36 N. Ueda, S.-I. Itoh, M. Tanaka and K. Itoh, *A Design Method of Divertor in Tokamak Reactors* Aug. 1990

NIFS-37 J. Todoroki, *Theory of Longitudinal Adiabatic Invariant in the Helical Torus*; Aug. 1990

NIFS-38 S.-I. Itoh and K. Itoh, *Modelling of Improved Confinements – Peaked Profile Modes and H-Mode–* ; Sep. 1990

NIFS-39 O. Kaneko, S. Kubo, K. Nishimura, T. Syoji, M. Hosokawa, K. Ida, H. Idei, H. Iguchi, K. Matsuoka, S. Morita, N. Noda, S. Okamura, T. Ozaki, A. Sagara, H. Sanuki, C. Takahashi, Y. Takeiri, Y. Takita, K. Tsuzuki, H. Yamada, T. Amano, A. Ando, M. Fujiwara, K. Hanatani, A. Karita, T. Kohmoto, A. Komori, K. Masai, T. Morisaki, O. Motojima, N. Nakajima, Y. Oka, M. Okamoto, S. Sobhanian and J. Todoroki, *Confinement Characteristics of High Power Heated Plasma in CHS*; Sep. 1990

NIFS-40 K. Toi, Y. Hamada, K. Kawahata, T. Watari, A. Ando, K. Ida, S. Morita, R. Kumazawa, Y. Oka, K. Masai, M. Sakamoto, K. Adati, R. Akiyama, S. Hidekuma, S. Hirokura, O. Kaneko, A. Karita, T. Kawamoto, Y. Kawasumi, M. Kojima, T. Kuroda, K. Narihara, Y. Ogawa, K. Ohkubo, S. Okajima, T. Ozaki, M. Sasao, K. Sato, K.N. Sato, T. Seki, F. Shimpo, H. Takahashi, S. Tanahashi, Y. Taniguchi and T. Tsuzuki, *Study of Limiter H- and IOC- Modes by Control of Edge Magnetic Shear and Gas Puffing in the JIPP T-IIU Tokamak*; Sep. 1990

NIFS-41 K. Ida, K. Itoh, S.-I. Itoh, S. Hidekuma and JIPP T-IIU & CHS Group, *Comparison of Toroidal/Poloidal Rotation in CHS Heliotron/Torsatron and JIPP T-IIU Tokamak*; Sep .1990

NIFS-42 T.Watari, R.Kumazawa,T.Seki, A.Ando,Y.Oka, O.Kaneko, K.Adati, R.Ando, T.Aoki, R.Akiyama, Y.Hamada, S.Hidekuma, S.Hirokura, E.Kako, A.Karita, K.Kawahata, T.Kawamoto, Y.Kawasumi, S.Kitagawa, Y.Kitoh, M.Kojima, T. Kuroda, K.Masai, S.Morita, K.Narihara, Y.Ogawa, K.Ohkubo, S.Okajima, T.Ozaki, M.Sakamoto, M.Sasao, K.Sato, K.N.Sato, F.Shinbo, H.Takahashi, S.Tanahashi, Y.Taniguchi, K.Toi, T.Tsuzuki, Y.Takase, K.Yoshioka, S.Kinoshita, M.Abe, H.Fukumoto, K.Takeuchi, T.Okazaki and M.Ohtuka, *,Application of Intermediate Frequency Range Fast Wave to JIPP T-IIU and HT-2 Plasma*; Sep. 1990

NIFS-43 K.Yamazaki, N.Ohyabu, M.Okamoto, T.Amano, J.Todoroki, Y.Ogawa, N.Nakajima, H.Akao, M.Asao, J.Fujita, Y.Hamada, T.Hayashi, T.Kamimura, H.Kaneko, T.Kuroda, S.Morimoto, N.Noda, T.Obiki, H.Sanuki, T.Sato, T.Satow, M.Wakatani, T.Watanabe, J.Yamamoto, O.Motojima, M.Fujiwara, A.Iiyoshi and LHD Design Group, *Physics Studies on Helical Confinement Configurations with l=2 Continuous Coil Systems*; Sep. 1990

NIFS-44 T.Hayashi, A.Takei, N.Ohyabu, T.Sato, M.Wakatani, H.Sugama, M.Yagi, K.Watanabe, B.G.Hong and W.Horton, *Equilibrium Beta Limit and Anomalous Transport Studies of Helical Systems*; Sep. 1990

NIFS-45 R.Horiuchi, T.Sato, and M.Tanaka, *Three-Dimensional Particle Simulation Study on Stabilization of the FRC Tilting Instability*;

Sep. 1990

NIFS-46 K.Kusano, T.Tamano and T. Sato, *Simulation Study of Nonlinear Dynamics in Reversed-Field Pinch Configuration*; Sep. 1990

NIFS-47 Yoshi H.Ichikawa, *Solitons and Chaos in Plasma*; Sep. 1990

NIFS-48 T.Seki, R.Kumazawa, Y.Takase, A.Fukuyama, T.Watari, A.Ando, Y.Oka, O.Kaneko, K.Adati, R.Akiyama, R.Ando, T.Aoki, Y.Hamada, S.Hidekuma, S.Hirokura, K.Ida, K.Itoh, S.-I.Itoh, E.Kako, A. Karita, K.Kawahata, T.Kawamoto, Y.Kawasumi, S.Kitagawa, Y.Kitoh, M.Kojima, T.Kuroda, K.Masai, S.Morita, K.Narihara, Y.Ogawa, K.Ohkubo, S.Okajima, T.Ozaki, M.Sakamoto, M.Sasao, K.Sato, K.N.Sato, F.Shinbo, H.Takahashi, S.Tanahashi, Y.Taniguchi, K.Toi and T.Tsuzuki, *Application of Intermediate Frequency Range Fast Wave to JIPP T-IIU Plasma*; Sep.1990

NIFS-49 A.Kageyama, K.Watanabe and T.Sato, *Global Simulation of the Magnetosphere with a Long Tail: The Formation and Ejection of Plasmoids*; Sep.1990

NIFS-50 S.Koide, *3-Dimensional Simulation of Dynamo Effect of Reversed Field Pinch*; Sep. 1990

NIFS-51 O.Motojima, K. Akaishi, M.Asao, K.Fujii, J.Fujita, T.Hino, Y.Hamada, H.Kaneko, S.Kitagawa, Y.Kubota, T.Kuroda, T.Mito, S.Morimoto, N.Noda, Y.Ogawa, I.Ohtake, N.Ohyabu, A.Sagara, T. Satow, K.Takahata, M.Takeo, S.Tanahashi, T.Tsuzuki, S.Yamada, J.Yamamoto, K.Yamazaki, N.Yanagi, H.Yonezu, M.Fujiwara, A.Iiyoshi and LHD Design Group, *Engineering Design Study of Superconducting Large Helical Device*; Sep. 1990

NIFS-52 T.Sato, R.Horiuchi, K. Watanabe, T. Hayashi and K.Kusano, *Self-Organizing Magnetohydrodynamic Plasma*; Sep. 1990

NIFS-53 M.Okamoto and N.Nakajima, *Bootstrap Currents in Stellarators and Tokamaks*; Sep. 1990

NIFS-54 K.Itoh and S.-I.Itoh, *Peaked-Density Profile Mode and Improved Confinement in Helical Systems*; Oct. 1990

NIFS-55 Y.Ueda, T.Enomoto and H.B.Stewart, *Chaotic Transients and Fractal Structures Governing Coupled Swing Dynamics*; Oct. 1990

NIFS-56 H.B.Stewart and Y.Ueda, *Catastrophes with Indeterminate Outcome*; Oct. 1990

NIFS-57 S.-I.Itoh, H.Maeda and Y.Miura, *Improved Modes and the Evaluation of Confinement Improvement*; Oct. 1990

NIFS-58 H.Maeda and S.-I.Itoh, *The Significance of Medium- or Small-size Devices in Fusion Research*; Oct. 1990

NIFS-59 A.Fukuyama, S.-I.Itoh, K.Itoh, K.Hamamatsu, V.S.Chan, S.C.Chiu, R.L.Miller and T.Ohkawa, *Nonresonant Current Drive by RF Helicity Injection*; Oct. 1990

NIFS-60 K.Ida, H.Yamada, H.Iguchi, S.Hidekuma, H.Sanuki, K.Yamazaki and CHS Group, *Electric Field Profile of CHS Heliotron/Torsatron Plasma with Tangential Neutral Beam Injection*; Oct. 1990

NIFS-61 T.Yabe and H.Hoshino, *Two- and Three-Dimensional Behavior of Rayleigh-Taylor and Kelvin-Helmholz Instabilities*; Oct. 1990

NIFS-62 H.B. Stewart, *Application of Fixed Point Theory to Chaotic Attractors of Forced Oscillators;* Nov. 1990

NIFS-63 K.Konn., M.Mituhashi, Yoshi H.Ichikawa,*Soliton on Thin Vortex Filament;* Dec. 1990

NIFS-64 K.Itoh, S.-I.Itoh and A.Fukuyama,*Impact of Improved Confinement on Fusion Research;* Dec. 1990

NIFS -65 A.Fukuyama, S.-I.Itoh and K. Itoh,*A Consistency Analysis on the Tokamak Reactor Plasmas;* Dec. 1990

NIFS-66 K.Itoh, H. Sanuki, S.-I. Itoh and K. Tani,*Effect of Radial Electric Field on α-Particle Loss in Tokamaks;* Dec. 1990

NIFS-67 K.Sato,and F.Miyawaki,*Effects of a Nonuniform Open Magnetic Field on the Plasma Presheath*; Jan.1991

NIFS-68 K.Itoh and S.-I.Itoh,*On Relation between Local Transport Coefficient and Global Confinement Scaling Law;* Jan. 1991

NIFS-69 T.Kato, K.Masai, T.Fujimoto,F.Koike, E.Källne, E.S.Marmar and J.E.Rice,*He-like Spectra Through Charge Exchange Processes in Tokamak Plasmas;* Jan.1991

NIFS-70 K. Ida, H. Yamada, H. Iguchi, K. Itoh and CHS Group, *Observation of Parallel Viscosity in the CHS Heliotron/Torsatron* ; Jan.1991

NIFS-71 H. Kaneko, *Spectral Analysis of the Heliotron Field with the Toroidal Harmonic Function in a Study of the Structure of Built-in Divertor* : Jan. 1991

NIFS-72 S. -I. Itoh, H. Sanuki and K. Itoh, *Effect of Electric Field Inhomogeneities on Drift Wave Instabilities and Anomalous Transport* ; Jan. 1991